



Soliton Chaos and Lengthscale Competition in Nonlinear Dynamics

RAINER SCHARF

Institut für Theoretische Physik, Universität Hannover, D-30167 Hannover, Germany

(Received 8 September 1993; revised 1 November 1993)

Abstract—Perturbing soliton-bearing completely integrable dynamics can give rise to rich and fascinating behaviour. If the perturbation introduces a lengthscale which is large compared to the spatial extent of the solitons present in the system, the solitons move like particles in an effective potential. Taking into account two-soliton interaction can result in chaotic behaviour called ‘soliton chaos’. In the opposite limit of a small-lengthscale perturbation the solitons acquire a dressing which effectively shields them from the perturbation. If the resulting ‘dressed solitons’ are subject to an additional long-wavelength perturbation they move like renormalised particles. Furthermore they can scatter nearly elastically. If the perturbation contains lengthscales which are comparable to one of the soliton’s typical lengthscales then lengthscale competition can occur. Neither the particle approximation nor the dressed-particle approximation for the soliton is valid and complicated spatio-temporal behaviour is observed. We illustrate this scenario by means of the perturbed nonlinear Schrödinger equation. The perturbed sine-Gordon equation and the Ablowitz-Ladik equation are also discussed.

1. INTRODUCTION

The presence of nonlinearity and spatial disorder in a physical system can lead to surprising effects [1] which can be of considerable relevance in applications, e.g. in nonlinear optics [2], long Josephson junctions [3], charge-density waves [4], polarons and bipolarons in polymers [5], dislocations in crystalline materials [6], solitary excitations in magnetic systems [7].

The best-studied spatially-extended nonlinear dynamics are $(1 + 1)$ -dimensional, like the nonlinear Schrödinger (NLS) equation, the ϕ^4 equation, and the sine-Gordon equation. Higher-dimensional systems have been studied mainly numerically (for analytical results see [8]). But often it is advantageous to start with an analytical approach. This brings completely integrable dynamics like the NLS equation and the sine-Gordon equation into focus. They can be solved by the inverse scattering method (see, for example [9]). The exact solutions of the unperturbed dynamics can then be used as a starting point to investigate the behaviour of more realistic dynamics modelled by adding perturbations to the completely-integrable dynamics. The extensive literature has been reviewed in [10, 11].

One lesson that could be learned from these results was that the success of the perturbative approach rests on the identification of the right starting point. Certain nonlinear excitations turned out to be extremely stable under certain forms of perturbations, while others were destroyed easily. This also gave a partial answer to the puzzling question of why completely integrable dynamics have any practical relevance at all. Or, as H. Segur put it recently [12]: ‘Who cares about integrability?’

The present article concentrates on a unifying theme common to many practical problems in one or more spatial dimensions, namely the occurrence of a distinguished lengthscale and its influence on the nonlinear excitations present in the systems. Here we

concentrate on $(1 + 1)$ -dimensional systems, but the lessons learned should be applicable to higher-dimensional systems as well.

The result can be stated in two sentences: When the localized nonlinear excitations and the perturbation live on very different lengthscales, then the excitations survive, appropriately modified. In the opposite case of competing lengthscales complicated spatio-temporal behaviour results, which usually is too involved for a simplified description.

When the lengthscales *are* different the dynamics often can be described in a simplified form by introducing collective variables. These variables describe the behaviour of the excitations of the perturbed system which resemble the unperturbed excitations like solitons and breathers.

Two cases have to be distinguished. Either the soliton's spatial extent is small compared to the perturbation's lengthscale, leading to a particle-like behaviour. Or the soliton is spread out over many wiggles of the perturbation leading to a 'dressed-particle' behaviour. These cases have been identified by numerical simulations using various dynamics. This will be the starting point for the analytical treatment that is reviewed in the present article.

The related situation of timescale competition can occur not only for driven systems but also for example in the case of optical solitons propagating in a fibre when the optical properties vary along the fibre. In this case the behaviour of the system is described by a NLS equation with the role of time and space exchanged [2]. Spatially fast periodic amplification of optical solitons, for example, can then be treated by a timescale separation in the NLS equation. This, together with a timescale separation analysis for other rapidly driven dynamics, is discussed by Kivshar and Spatschek [13] in the present issue.

We conclude the introduction with a short preview of the following sections. In Section 2 we discuss the 'particle limit' when the soliton's spatial extent is small compared to the characteristic lengthscales of the perturbing potential. In this case the soliton behaves like a particle moving in an effective potential depending on the position of the centre of the soliton. This is illustrated in 2.1 for the discrete NLS equation. The discreteness of the system gives rise to an unexpected localisation effect. In 2.2 we turn to the continuum NLS equation, derive the effective potential, investigate two-soliton interaction, and finally discuss the novel effect of 'soliton chaos' which results from the non-integrability of the pairwise interaction of solitons in the presence of a long-wavelength perturbation. In 2.3 we discuss the particle-like behaviour of sine-Gordon kinks, antikinks, and breathers in the presence of a certain type of perturbation. Again, chaotic behaviour or soliton chaos is found under certain conditions.

In Section 3 we investigate the 'dressed-particle limit' resulting from a short-wavelength perturbation acting on a soliton. In 3.1 we discuss the dressed-particle limit for the continuum NLS. Adding long-wavelength perturbations the dressed solitons move like particles in an effective potential. Surprisingly, even two-soliton collisions leave the dressed solitons intact, thereby illustrating that the dressing actually renormalises the perturbation, leading to a dynamics which involves only a small number of degrees of freedom for certain initial conditions. In 3.2 we discuss the dressed-particle limit for the sine-Gordon equation.

In Section 4 we turn to the interesting case of lengthscale competition. The competing lengthscales are the characteristic lengthscale of the soliton and of the perturbation it experiences. Lengthscale competition results in complicated spatio-temporal behaviour. Neither the particle nor the dressed-particle behaviour is observed. In 4.1 we show that for the continuum NLS essentially two situations of lengthscale competition can occur. In the first case, called 'phase resonance', the length of the phase modulation of the soliton sets the relevant scale. In the second case, called 'shape resonance', the spatial width of the soliton is the relevant lengthscale. In 4.2 lengthscale competition is discussed for the sine-Gordon breather. Here, only shape resonance in a very broad sense can occur. In all

these cases it is clearly seen that lengthscale competition strongly affects the stability of coherent non-topological excitations, eventually leading to a quick breakup into radiation or smaller localised excitations.

In Section 5 we conclude with some open questions.

2. THE PARTICLE LIMIT

If the width of a soliton is small compared to the length on which a perturbation becomes palpable, it is natural to neglect all degrees of freedom of the soliton besides its centre-of-mass motion and to treat it as a particle. The particle's position will be the collective coordinate describing the status of the underlying dynamics with its (infinitely) many degrees of freedom.

The use of collective coordinates has a long history. In the context of completely-integrable dynamics they were used in the study of semiclassical quantization of (1 + 1)-dimensional nonlinear field equations around nonlinear excitations. For an introduction see [14]. For the use of collective variables for classical field equations see, for example [15].

The advantage of a reduced description of the dynamics in terms of collective variables is obvious. After identifying the few relevant excitations in the system the description is focused on them, thereby bringing into play the powerful methods of classical (few) particle mechanics.

In contrast to the full dynamics, this reduced one-dimensional single-particle dynamics will still be integrable. It is governed by an effective Hamiltonian which can be determined by calculating the total energy of the soliton in the presence of the perturbation as a function of its position and velocity. An extension to two and more solitons is straightforward under the assumption that only two-soliton collisions occur. In the unperturbed case these collisions are elastic: the momenta of the solitons, as well as their shapes, are unchanged by the collision. In the reduced description this can be modelled by a two-particle interaction. In the case we will discuss, this interaction is attractive. Adding this interaction to the single-particle Hamiltonian results in a two- or more-particle Hamiltonian which is non-integrable in general. This can lead to 'soliton chaos' for certain initial conditions.

2.1. The discrete NLS equation

There are infinitely many spatial discretisations of the continuum NLS equation. A rich class of such discrete NLS equations, which describe for example the propagation of molecular excitations in a chain, was discussed in [16]. Only for one particular choice of parameters is the dynamics completely integrable and of the form introduced by Ablowitz and Ladik [17]. Here we use this particular model as a starting point for investigating the effect of perturbations on discrete nonlinear dynamics by adding an on-site potential V_n :

$$i\dot{\psi}_n = -(\psi_{n+1} + \psi_{n-1})(1 + |\psi_n|^2) + V_n\psi_n, \quad (1)$$

with the complex field ψ_n on lattice site n . The dot denotes the time derivative. The Hamiltonian has the form

$$H = -\sum_n (\psi_n \psi_{n+1}^* + \psi_n^* \psi_{n+1}) + \sum_n V_n \ln(1 + |\psi_n|^2). \quad (2)$$

For $V_n = 0$ there are infinitely many independent integrals of motion in involution with

each other and with H (see [17]). For general V_n only one of them (besides H) survives, the 'norm' N :

$$N = \sum_n \ln(1 + |\psi_n|^2). \quad (3)$$

It was shown in [18] that equation (1) is completely integrable for $V_n = V_0 + an$. In this case the soliton solutions are of the form

$$\psi_n(t) = \sinh \beta \operatorname{sech}(\beta(n - q(t))) \exp[-i(\phi(t) + \alpha(t)n)] \quad (4)$$

with real parameters $\alpha(t) = at + \alpha_0$ and β , a time-dependent phase ϕ , and the soliton position $q(t)$ (for details see [18]):

$$q(t) = (2/a\beta) \sinh \beta (\cos(at) - 1) + q_0. \quad (5)$$

The norm N and the energy of the soliton for linear V_n , can be determined exactly:

$$N = 2\beta, \quad (6)$$

$$E = -4 \sinh \beta \cos \alpha + NV(q), \quad (7)$$

with the potential $V(q) = V_0 + aq$ depending only on the position of the soliton.

For more general potentials we assume that the spatial extent of the soliton is sufficiently small compared to the typical distance of extrema of the potential so that the potential can be approximated locally linearly:

$$V_n \approx V(q) + V'(q)(n - q). \quad (8)$$

Then we find for the total energy the result (7). As the velocity of the soliton is given by

$$\dot{q} = -(2/\beta) \sinh \beta \sin \alpha \quad (9)$$

one can easily set up an effective single-particle Hamiltonian which governs the motion of the soliton in a general potential under the assumptions made:

$$H_{\text{eff}} = \frac{p^2}{2} + \frac{V(q)(\beta V(q) - E)}{2\beta} = \frac{16 \sin^2 \beta - E^2}{8\beta^2}, \quad (10)$$

where E is the energy of the soliton in contradistinction to the particle's energy H_{eff} . In the particle description the soliton experiences an effective potential which is quadratic in the original perturbation $V(q)$, thereby leading, for example, to harmonic behaviour in the case of a linear perturbation, which is illustrated in Fig. 1. For a general potential the soliton can be trapped between two maxima of the *effective* potential $V(\beta V - E)/2\beta$ with surprising effects in view of the bare potential V .

As the system is spatially discrete it has a maximum velocity for each soliton. Further acceleration leads to a decrease and to a sign-reversal of the soliton's velocity. In the limit of the continuum NLS, which is discussed next, this unusual feature vanishes.

2.2. The continuum NLS equation

We now turn to the NLS equation for the complex field $\psi(x, t)$ perturbed by an on-site potential:

$$i\psi_t + \psi_{xx} + 2\psi|\psi|^2 = \epsilon\psi V(x), \quad (11)$$

where subscripts t and x denote time and space derivatives. As in the case of the discrete

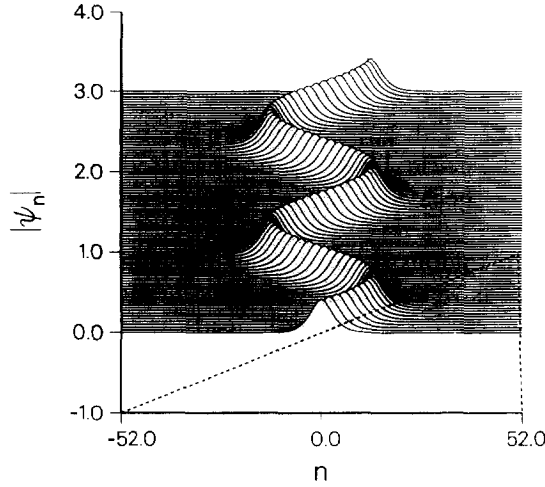


Fig. 1. A discrete NLS soliton trapped in a linear potential $V_n = 2n/13$. The initial soliton parameters: $\beta = 0.4$, $\alpha = -1.571$. The integration time $T = 90$. The dashed line indicates the (scaled) potential.

NLS the continuum NLS is completely integrable for perturbations $V(x)$ which are linear in x [19]. For general perturbations two integrals remain, the energy and the norm:

$$H = \int_{-\infty}^{+\infty} dx (|\psi_x|^2 - |\psi|^4 + \epsilon |\psi|^2 V(x)), \quad (12)$$

$$N = \int_{-\infty}^{+\infty} dx |\psi|^2. \quad (13)$$

We assume that the system contains only a single soliton and that the curvature of the potential experienced by the soliton is sufficiently small that the only mode excited by the perturbation is the translational mode. This means that the soliton only moves but does not change its shape or radiate. We therefore make an ansatz (in the spirit of [20]) for the single-soliton solution similar to the form of the unperturbed soliton (see [10]) but with time-dependent parameters q and Φ :

$$\psi(x, t) = 2i\eta \frac{\exp(i\dot{q}x/2 - i\Phi)}{\cosh(2\eta(x - q))}. \quad (14)$$

With the appropriate choice of $q(t)$ and $\Phi(t)$ this is the exact solution for the linear potential. The time-dependent phase Φ has no influence on the centre-of-mass motion of single soliton. Only for soliton collisions in the presence of a perturbation a relative phase can be important. Concentrating on single-soliton motion we therefore neglect this phase.

The norm of the soliton is given by $N = 4\eta$. The soliton's total energy depends only on its position and velocity:

$$H = \eta(\dot{q}^2 - \frac{16}{3}\eta^2) + V_{\text{eff}}(q) \quad (15)$$

with the effective potential

$$V_{\text{eff}}(q) = 4\eta^2 \epsilon \int_{-\infty}^{+\infty} dx \operatorname{sech}^2(2\eta(x - q)) V(x). \quad (16)$$

We identify the effective mass of the soliton: $m = 2\eta = N/2$. Skipping a constant term of the Hamiltonian we find the effective Hamiltonian for the soliton:

$$H_{\text{eff}}(q) = (p^2/2m) + V_{\text{eff}}(q). \quad (17)$$

For a cosine potential $V(x) = \cos(kx)$ one calculates:

$$V_{\text{eff}}(q) = \frac{\epsilon\pi k}{\sinh(k\pi/4\eta)} \cos(kq). \quad (18)$$

Obviously the Fourier modes with large k are exponentially suppressed. This fact will be important in the 'dressed-particle limit' to be discussed in the next section. Figure 2 illustrates the particle-like behaviour of a single soliton in a cosine potential with $k\pi/4\eta \approx 1/3$.

What happens when two solitons collide? After the collision the solitons re-emerge with their parameters η_1 and η_2 as well as their velocities v_1 and v_2 unchanged. But the solitons attract each other, and therefore their collision leads to spatial shifts. For the soliton that was on the right side initially:

$$\lim_{t \rightarrow \pm\infty} |\psi| = \text{sech}(2\eta(x - vt) \pm a). \quad (19)$$

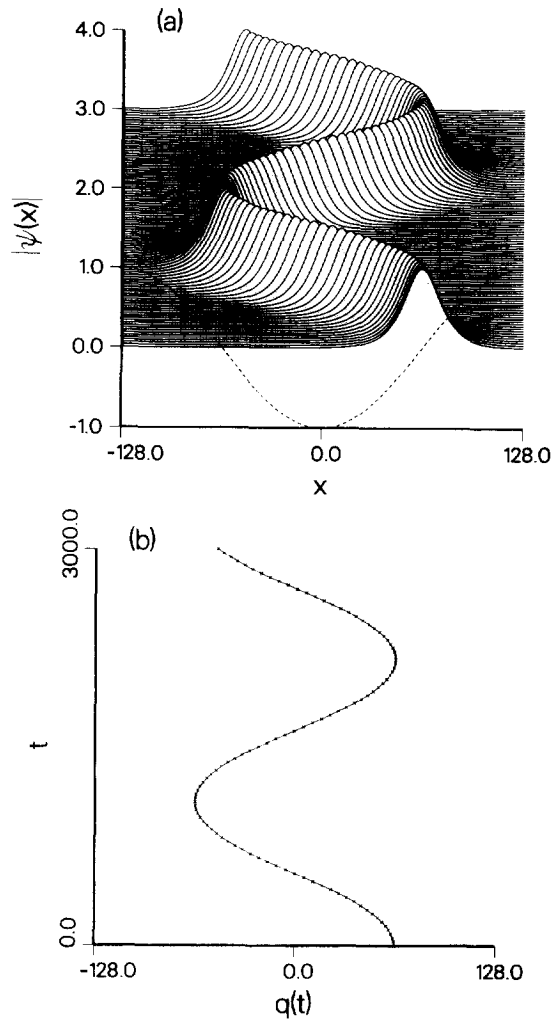


Fig. 2. A single NLS soliton moving in the potential $\epsilon V(x) = -\cos(2\pi x/256)/100$. (a) The full NLS dynamics. (b) Comparison between the soliton track (full line) and the effective particle dynamics (crosses). Initial soliton parameters: $\dot{q} = 0$, $\eta = 0.05$, $x_0 = 64$. Total integration time $T = 3000$.

For the soliton that was on the left side initially the shift a should be replaced by $-a$. The shift is given by [21]:

$$a = \frac{1}{2} \ln \left(\frac{16(\eta_1 + \eta_2)^2 + (v_1 - v_2)^2}{16(\eta_1 - \eta_2)^2 + (v_1 - v_2)^2} \right). \quad (20)$$

For $4|\eta_1 - \eta_2| \leq |v_1 - v_2|$ an attractive two-particle potential can be found which gives rise to the correct spatial shifts for arbitrary initial conditions:

$$V_{12}(q) = -16\eta_1\eta_2(\eta_1 + \eta_2) \operatorname{sech}^2 \left(\frac{2\eta_1\eta_2q}{\eta_1 + \eta_2} \right). \quad (21)$$

Collecting all terms we find an expression for the effective Hamiltonian which describes the particle-like behaviour of two solitons in the presence of a perturbation $V(x)$ and takes into account collisions with sufficiently large relative velocity:

$$H_{\text{eff}} = \frac{p_1^2}{4\eta_1} + \frac{p_2^2}{4\eta_2} + V_{\text{eff}}(q_1) + V_{\text{eff}}(q_2) + V_{12}(q_1 - q_2). \quad (22)$$

In Fig. 3 we illustrate the effect of the two-soliton interaction V_{12} in the absence of an external perturbation ($V_{\text{eff}} = 0$) for periodic boundary conditions. Figure 4 shows the same but with an effective cosine potential. A generalisation to more than two solitons is straightforward.

Several effects limit the validity of the particle description for two-soliton collisions given by equation (22). When three or more solitons meet simultaneously in the presence of a perturbation, the spatial shifts calculated from the particle dynamics show deviations from the shifts of the solitons found by numerically integrating the full perturbed NLS equation. This happens for perturbations and initial conditions for which two-soliton collisions are well described by the effective two-particle dynamics. But even for two-soliton collisions strong deviations between the full NLS dynamics and the predictions of the effective particle dynamics can occur. If the solitons collide with small or vanishing relative velocity the spatial shifts derived from the effective two-particle dynamics no longer agree with the exact two-soliton shifts given by equation (20). In addition, inelastic effects have been observed, leading to a change of the amplitude parameters η_1 and η_2 during the collision. An example is given in Fig. 5.

In a dilute gas of N solitons all these effects have negligible probability. Therefore we expect an N -particle description with an effective N -particle Hamiltonian instead of the two-particle Hamiltonian (22) to be valid in this limit.

The non-integrability of the perturbed NLS equation can be established already by inspecting the effective two-particle dynamics. If the perturbation leads to non-integrable behaviour already in this case then the full perturbed NLS equation cannot be integrable either. With $V(x) = \cos(kx)$ for example the two-particle dynamics turns out to be non-integrable.

Under appropriate initial conditions chaotic motion of the solitons can be observed. This behaviour was called ‘soliton chaos’ and has been investigated in [22]. Chaotic motion of solitons has already been observed in driven systems (for a review see [23]). We want to stress that the novel feature of ‘soliton chaos’ is that it occurs in autonomous systems. The non-integrability of the perturbed dynamics becomes manifest already in the two-soliton sector either as chaotic two-particle motion for spatially periodic boundary conditions or as chaotic scattering for spatially unbounded systems. For sufficiently small perturbation the generation of radiation can be made arbitrarily small on correspondingly longer timescales.

Chaotic motion of solitons can give rise to diffusive transport of excitation in the system. In Fig. 6 we show how a soliton initially pinned in a potential minimum is periodically excited by fast solitons ultimately leading to depinning and Brownian motion of the soliton.

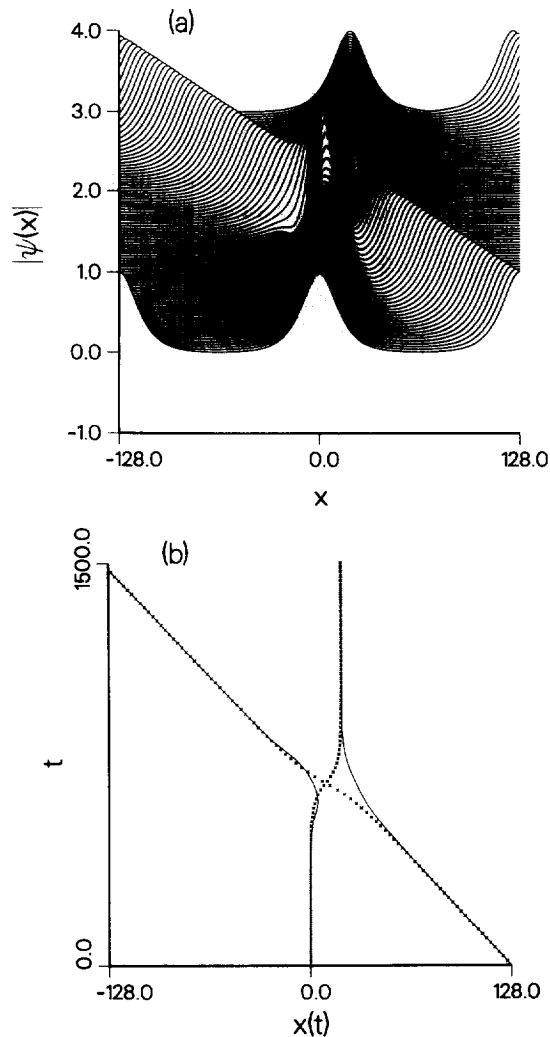


Fig. 3. Two NLS solitons colliding without onsite potential. (a) The full dynamics. (b) The soliton tracks in comparison with the particle dynamics. Periodic boundary conditions. Total integration time $T = 1500$. Initial soliton parameters: $\dot{q} = 0$, $\dot{q}_2 = -0.16$, $\eta_1 = \eta_2 = 0.05$.

2.3. The sine-Gordon equation

The literature about the sine-Gordon equation with conservative, dissipative, or time-dependent perturbations is considerable (for an overview see [10, 11]). Here we concentrate on a particular form of conservative perturbation which introduces an additional lengthscale in the system.

If a spatially discrete system can carry topological excitations which are sufficiently extended in space, then a continuum description can be a good starting point. For an effectively one-dimensional system ϕ^4 or sine-Gordon equation are well-investigated models for this case. If one wants to improve the model by taking into account the underlying lattice structure without sacrificing the continuum description, one can add a spatially-periodic perturbation with a period on the lengthscale of the lattice constant. In the case of a ϕ^4 -kink travelling in a periodic perturbation, a shape mode is excited which can modulate the velocity of the kink or even lead to trapping [24].

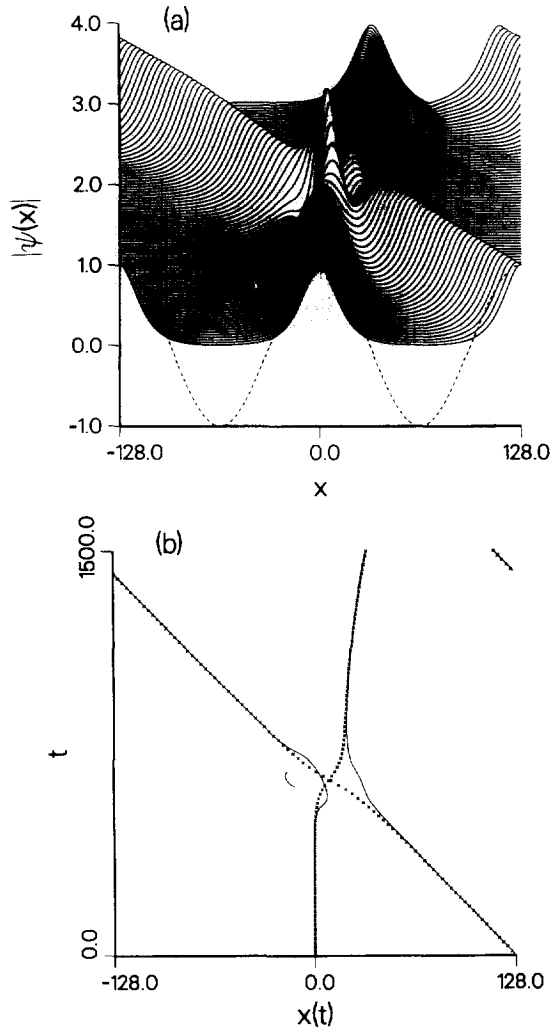


Fig. 4. Two NLS solitons colliding on the potential: $\epsilon V(x) = \cos(2\pi x/128)/2000$. (a) The full dynamics. (b) The soliton tracks in comparison with the particle dynamics. Total integration time $T = 1500$. Initial soliton parameters are the same as in Fig. 3.

A different route is to investigate lattice models directly, like the discrete ϕ^4 [25] or the discrete sine-Gordon equation [26].

For semiconductor superlattices one can vary the lengthscale of periodic modulations of electronic or magnetic features over a large range. This can be modelled by spatially periodic perturbations, too. In this case the added lengthscale can be large, equal, or small compared to the spatial extent of the excitations.

As we want to use a completely-integrable dynamics as a starting point we restrict the perturbations to those that locally change the features of the dynamics as little as possible. In the case of the sine-Gordon equation we want to leave the vacuum state unchanged under the perturbation. This leads to a Hamiltonian of the form:

$$H = \int_{-\infty}^{+\infty} dx \left(\frac{1}{2} u_t^2 + \frac{1}{2} u_x^2 + (1 + \epsilon \cos(kx))(1 - \cos u) \right), \quad (23)$$

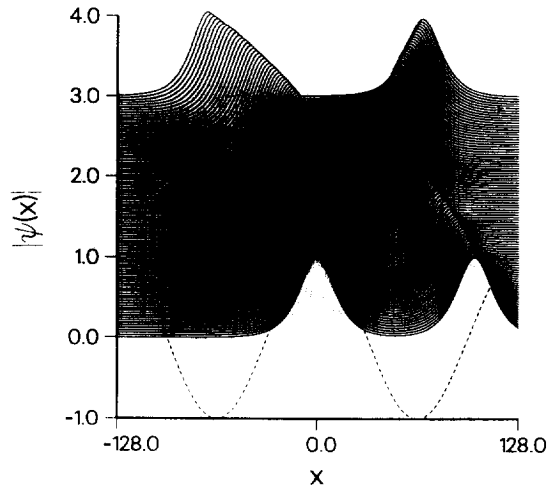


Fig. 5. Inelastic collision of two NLS solitons with equal initial amplitudes in the presence of a potential (same as in Fig. 4). Note the different amplitudes after the collision. Total integration time $T = 2000$. Initial soliton parameters: $\dot{q}_1 = 0$, $\dot{q}_2 = -0.02$, $\eta_1 = \eta_2 = 0.05$.

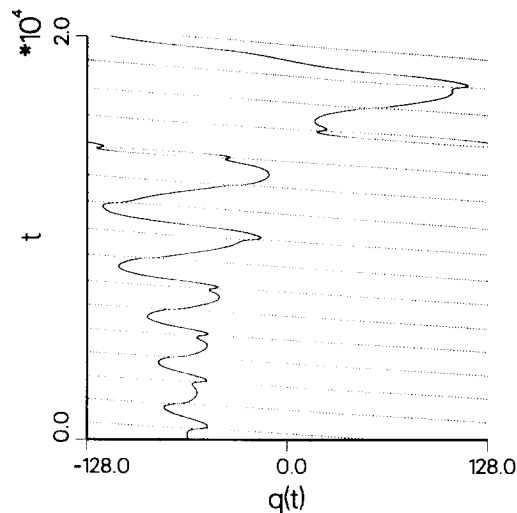


Fig. 6. Chaotic two-particle dynamics modelling soliton chaos in the presence of the potential $\epsilon V(x) = \cos(2\pi x/128)/500$. Periodic boundary conditions. Shown are the tracks of a fast and a slow soliton. Initial soliton parameters: $\dot{q}_1 = 0$, $\dot{q}_2 = -0.23$, $\eta_1 = \eta_2 = 0.2$.

with the real field $u(x, t)$. For $\epsilon = 0$ the sine-Gordon Hamiltonian is recovered. For $|\epsilon| < 1$ we note that the groundstate of the perturbed dynamics is still the unperturbed vacuum $u \equiv 0 \pmod{2\pi}$. But the Lorentz covariance and the translational invariance of the unperturbed dynamics is lost. We will restrict our discussion to the 'non-relativistic' limit (with $v \ll c = 1$).

From equation (23) one derives the equation of motion

$$u_{tt} - u_{xx} + (1 + \epsilon \cos(kx)) \sin u = 0. \quad (24)$$

For $\epsilon \neq 0$ this equation is no longer integrable. Numerical simulations show that this simple

perturbation can lead to very complicated behaviour in space and time. A general description of this behaviour in analytic terms seems no longer possible nor appropriate. Instead, we will concentrate on certain limiting cases with sufficiently simple behaviour which can be described by collective coordinates.

2.3.1. *Kinks and antikinks.* As is well known the sine–Gordon equation possesses two types of topological soliton solutions, kinks and antikinks:

$$u(x, t) = 4 \arctan [\exp \pm \{\gamma(x - vt)\}] \quad (25)$$

with $\gamma = 1/\sqrt{1 - v^2}$. The centre of the kink or antikink is located at $q(t) = vt$. Using equation (23) the energy of a kink (or antikink) placed on the perturbing potential is given by:

$$E_K = 8\gamma + \frac{2\epsilon k\pi}{\gamma^2 \sinh(k\pi/2\gamma)} \cos(kq). \quad (26)$$

A general solution of the unperturbed sine–Gordon equation will experience the influence of the cosine potential leading to complicated behaviour in general. On the other hand, the conservation of the topological charge prevents kinks and antikinks from decaying into the vacuum by emitting radiation. This leads to their amazing stability even under very strong perturbations with $\epsilon = O(1)$ which has been observed numerically.

The influence of a perturbation on a kink can be analysed in terms of mode excitation. The excitation of radiative modes in the case of the perturbed sine–Gordon equation has been treated perturbatively (for references see [10]). Here we concentrate on modes trapped on the soliton. If the wavelength of the perturbation ($\lambda = 2\pi/k$) is large compared to the width of the soliton, then only translational and shape modes are relevant. In the (non-integrable) case of the ϕ^4 -kinks shape modes can be excited for example by kink–antikink collisions [27]. For the somewhat similar case of sine–Gordon kinks interacting with impurity modes see [28]. For isolated sine–Gordon kinks only the translational mode is relevant, and in the non-relativistic limit kinks move like particles in an effective potential. For $v^2 \ll 1$ we set $p = m_0 v$ with $m_0 = 8$ denoting the (anti-)kink's rest mass and derive from equation (26) the effective non-relativistic Hamiltonian for a single (anti-)kink:

$$H_K = \frac{p^2}{2m_0} + V_{\text{eff}}(q) + m_0, \quad (27)$$

with the effective potential:

$$V_{\text{eff}}(q) = \frac{2\pi\epsilon k}{\sinh(\pi k/2)} \cos(kq). \quad (28)$$

Kinks and antikinks of the perturbed sine–Gordon dynamics (24) move like particles in a rescaled cosine-potential which should be compared with the result (18) for the perturbed NLS equation. Again the large- k perturbations are exponentially suppressed.

2.3.2 *Kink–antikink collision.* Kinks and antikinks of the sine–Gordon equation scatter elastically. Their asymptotic momenta are unchanged, but their attraction leads to a spatial shift. This can be discussed using the exact kink–antikink solution:

$$u(x, t) = 4 \arctan \left(\frac{\sinh(\gamma\gamma'(t - vx)v')}{v' \cosh(\gamma\gamma'(x - vt - x_0))} \right), \quad (29)$$

with v denoting the centre-of-mass velocity of the kink–antikink pair, $\gamma = 1/\sqrt{1 - v^2}$, and

γ' correspondingly for the relative velocity v' . This solution can be decomposed exactly into kink and antikink in the following way (see, for example [29]):

$$u(x, t) = 4 \arctan(\exp \gamma \gamma'(x + z - vt - x_0)) - 4 \arctan(\exp \gamma \gamma'(x - z - vt - x_0)). \quad (30)$$

The distance $2z$ between kink and antikink in the centre-of-mass frame is given by:

$$\sinh(\gamma \gamma' z) = \sinh(\gamma \gamma'(t - vx)v'/v'). \quad (31)$$

When kink and antikink are infinitely far apart they have the velocities:

$$v_{1,2} = \gamma \gamma'(v \pm v'). \quad (32)$$

After transformation to the centre-of-mass frame ($v = 0$) we restrict our discussion to the nonrelativistic limit ($v' \ll 1$). From equation (31) one can easily derive the effective interaction between kink and antikink:

$$V_{12}(q) = -2 \operatorname{sech}^2(q/2), \quad (33)$$

leading to the effective kink–antikink Hamiltonian in the non-relativistic limit (upon skipping the rest mass)

$$H_{\kappa \bar{\kappa}} = \sum_{i=1}^2 \left(\frac{1}{2m_0} p_i^2 + V_{\text{eff}}(q_i) \right) + V_{12}(q_1 - q_2). \quad (34)$$

It has essentially the same form as the two-soliton Hamiltonian (22) for the perturbed NLS equation. Therefore we expect soliton chaos to occur for kink and antikink interacting in a long-wavelength potential.

In [30] the situation of an effective potential competing with the attractive kink–antikink interaction was discussed. When kink and antikink are near a sufficiently deep minimum of the effective potential a breather can be formed. Using the total potential energy of the kink–antikink pair the threshold for breather creation could be determined. For details see [30]. Furthermore, it was observed numerically that during the collision kink and antikink are much more susceptible to the perturbation than the independent solitons. This effect will be discussed in the next Section.

2.3.3. Breather breakup. Kinks and antikinks attract each other and can form bound states called breathers if their total energy is sufficiently small. A perturbing potential can change the total energy of a kink–antikink pair and thereby lead either to a splitting of the breather into free kink and antikink or to a trapping of the otherwise free kink and antikink into a breather. We calculated the energy of a breather at rest in the presence of the perturbation and used the result to derive a threshold for breather breakup [30].

An unperturbed sine–Gordon breather at rest has the form:

$$u(x, t) = 4 \arctan \left(\tan \mu \frac{\sin((t - t_0) \cos \mu)}{\cosh((x - x_0) \sin \mu)} \right). \quad (35)$$

The parameter μ governs the breather's shape, size and frequency. For $\mu \rightarrow 0$ the breather becomes shallower, its frequency $\omega = \cos \mu$ grows and it essentially behaves like a NLS soliton. For $\mu \rightarrow \pi/2$ the breather approaches the case of a free kink–antikink pair and its frequency goes to zero. In the unperturbed case the total energy $E = 2m_0 = 16$ is the boundary between breathers (below) and free pairs (above). A perturbation can change

this boundary locally. The breakup situation is characterised by a maximum of the total potential energy:

$$E_{\text{pot}} = \int_{-\infty}^{+\infty} dx \left[\frac{1}{2} u_x^2 + (1 + \epsilon \cos(kx))(1 - \cos u) \right]. \quad (36)$$

In the absence of the perturbation ($\epsilon = 0$) the potential energy has one global minimum, namely when the kink and antikink annihilate ($t = t_0$) and all its energy is kinetic. The perturbation can generate new minima. The maxima in the immediate vicinity of the global minimum determine the critical initial conditions dividing the regimes of intact breathers and of breakup into kink and antikink. Details can be found in [30]. In Fig. 7 we illustrate the behaviour of breathers with initial conditions below and above the threshold.

2.3.4. Particle-like behaviour for breathers A breather consists of a bound kink-antikink pair. In a long-wavelength potential it therefore behaves like a particle with an internal degree of freedom. Near the breakup threshold, where the breather splits into kink

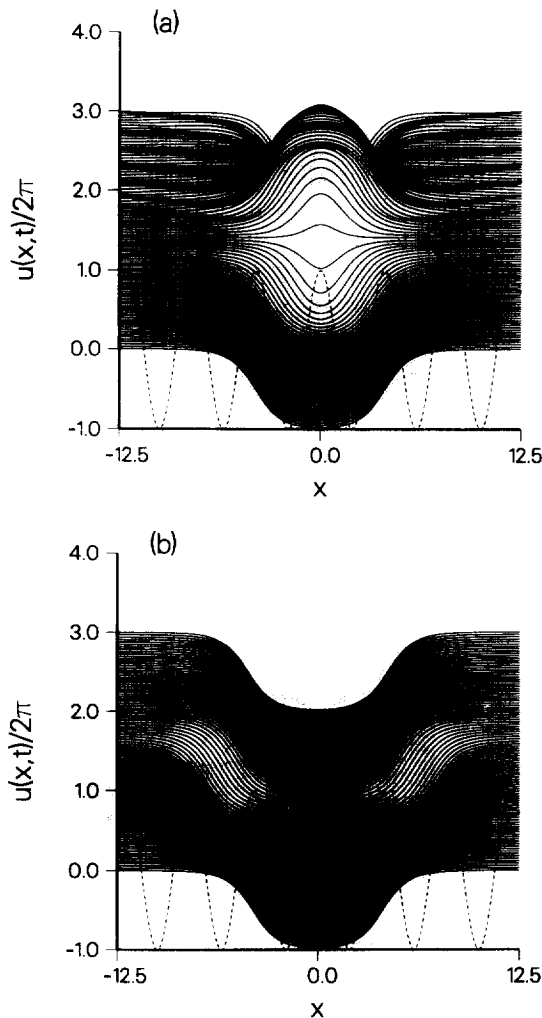


Fig. 7. Break-up of sine-Gordon breathers induced by the potential $\epsilon V(x) = \cos(\pi x/2)/10$. (a) Breather below breakup threshold ($\mu = 1.535$). (b) Slightly above breakup threshold ($\mu = 1.536$).

and antikink, chaotic behaviour associated with a homoclinic tangle can be observed. In the opposite case when the centre-of-mass motion decouples from the internal degree of freedom the breather moves like a simple particle in an effective potential as is illustrated in Fig. 8. More details can be found in [30, 31].

3. THE DRESSED-PARTICLE LIMIT

So far we have addressed the case when localised excitations have a spatial extent much smaller than the typical lengthscale of the perturbing potential. Now we turn to the opposite limit, when a soliton covers many wiggles of the perturbation. Hasegawa and Kodama [32] analysed this problem for NLS solitons showing that the averaged ‘guiding centre’ soliton behaves rather robustly. They used very general but quite complicated Lie techniques. We favour a more simple-minded approach originally devised by Kapitza for solving the problem of a particle moving in a rapidly oscillating field (see [33]).

We assume that a separation of lengthscales should be possible into a ‘slow’ spatial scale related to the soliton and a ‘fast’ scale related to the perturbation. Numerical simulations show that this approach is essentially correct. The related case of the NLS equation with amplification periodic in time was treated in a similar spirit in [34] (see also [13]).

3.1. The continuum NLS equation

Numerical simulations first revealed that NLS solitons with sufficiently large spatial extension propagating over very small-wavelength perturbations tend to smooth over the short lengthscales. In comparison to the unperturbed solitons they acquire a ‘dressing’ with the wavelength of the monochromatic perturbation [35]. In the polychromatic case the dressing is a sum of monochromatic dressings.

We first discuss the monochromatic case:

$$iu_t + u_{xx} + 2u|u|^2 = \epsilon u \cos(kx), \quad (37)$$

with $k \ll 1$ and make an ansatz of the form:

$$u(x, t) = \psi(x, t)(1 + \chi(kx, t)), \quad (38)$$

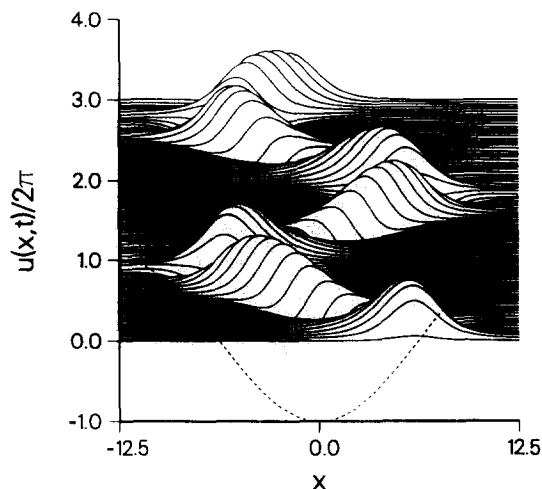


Fig. 8. Particle-like behaviour of sine-Gordon breathers in the potential $\epsilon V(x) = -\cos(2\pi x/25)/2$. Breather initially at rest and with $\mu = 1$.

where we assume that the ‘envelope’ $\psi(x, t)$ depends on x only ‘slowly’, i.e. that it involves only parameters small compared to k . It will turn out that $|\chi| = O(1/k^2)$. Therefore we linearise equation (37) with respect to χ . Besides the ‘slow’ dependence the resulting equation depends on the fundamental kx and on higher harmonics. The zero Fourier mode therefore gives an evolution equation for the slow part:

$$i\psi_t + \psi_{xx} + 2\psi|\psi|^2 = \epsilon\psi\langle\chi\cos(kx)\rangle. \quad (39)$$

This is the unperturbed NLS equation with a frequency shifted by the spatial average $\epsilon\langle\chi\cos(kx)\rangle$. The solution of this renormalised NLS equation is given by equation (14) with $\dot{q} = 0$ and an appropriately chosen phase Φ . Introducing $z = kx$ one finds for the next order:

$$2k\chi_z\psi_x + k^2\chi_{zz}\psi = \epsilon\psi\cos(kx), \quad (40)$$

which is solved to leading order by:

$$\chi(x, t) = -\epsilon k^{-2}\cos(kx), \quad (41)$$

in agreement with the assumption on χ made earlier. Relaxing the conditions on the soliton parameters a little bit and allowing for a large soliton velocity ($\dot{q} = O(k)$) but with $|\dot{q}^2 - k^2| = O(k^2)$ one calculates

$$\chi(x, t) = -\frac{\epsilon\cos(kx)}{k^2 - \dot{q}^2} + \frac{i\epsilon\dot{q}\sin(kx)}{k(k^2 - \dot{q}^2)}. \quad (42)$$

What do these modulations of the unperturbed frequency-shifted soliton look like? To leading order one has:

$$|1 + \chi(kx, t)|^2 = 1 - \frac{2\epsilon\cos(kx)}{k^2 - \dot{q}^2}. \quad (43)$$

For solitons at rest or moving with small velocity ($|\dot{q}| < k$) the shape modulations have a phase difference π relative to the perturbation. Maxima of the modulation are located at minima of the perturbation and vice versa. For fast solitons ($|\dot{q}| > k$) the modulations and the perturbation are in phase. The resonant case will be discussed in the next Section. In Fig. 9 this is shown for modulated or ‘dressed’ solitons with small and large velocities travelling on a large- k cosine potential.

The generalisation to finitely many short-lengthscale perturbations of the form $V(x) = \sum_i \epsilon_i \cos(k_i x)$ is easily achieved leading to a multicolour modulation summing over terms of the form (42), where all ϵ_i as well as all k_i are assumed to be of the same order, respectively.

The modulation χ can be interpreted as a ‘dressing’ that shields the soliton against the fast modulations of the perturbing potential. The resulting ‘dressed’ soliton in the monochromatic case has the form of an unperturbed soliton with a mode trapped on top of it. In the absence of the soliton this mode is not able to propagate as its group velocity vanishes.

Adding a long-wavelength perturbation $V_0(x)$ to the fast perturbation $\epsilon\cos(kx)$ will lead to particle-like behaviour of the dressed soliton under the same conditions as for the bare soliton case with $V(x) = V_0(x)$. We can calculate the norm and the effective potential under the assumption that the bare soliton’s parameters η and \dot{q} are both small compared with the wavenumber $k \ll 1$. We find that both the norm as well as the energy are given by the corresponding values for the bare solitons when one neglects terms which are small compared to ϵ^2/k^2 . Within the order of approximation we considered the dressed soliton is shielded completely from the large- k perturbations. Its motion under the long-wavelength

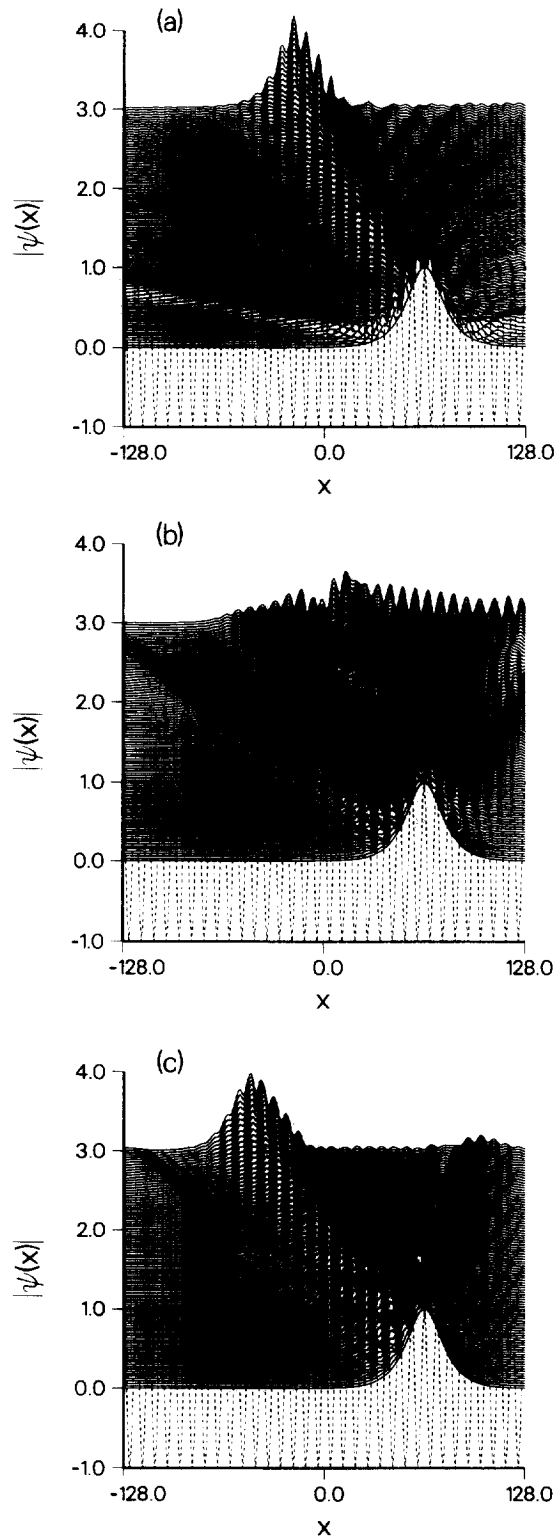


Fig. 9. Dressed NLS solitons ($\eta = 0.05$) (a) with small velocity ($\dot{q} = -0.2$), (b) resonant velocity ($\dot{q} = -0.8$), and (c) large velocity ($\dot{q} = -1.2$) propagating over a cosine perturbation ($\epsilon = 0.1$, $k = 0.785$).

perturbation is governed by the same effective Hamiltonian (15) as the motion of the bare soliton. This is illustrated in Fig. 10 which should be compared with Fig. 2.

Numerical simulations show that the shielding of dressed solitons from the ‘fast’ perturbations is so effective that they collide essentially like bare solitons in the absence of the perturbation. The comparison of the collision of two bare unperturbed solitons with the collision of two dressed solitons in the presence of a perturbation in Fig. 11 reveals striking similarities.

It should be noted that the small parameter in the problem is ϵ/k which shows that the lengthscale separation works even for relatively strong perturbations ($\epsilon > 1$) as long as $k \gg \epsilon$.

3.2. The sine–Gordon equation

The effect of a short-wavelength perturbation on a localised sine–Gordon excitation like kink, antikink or breather can be calculated in a similar way as for the NLS case. Therefore we can be brief. Starting from equation (24) with $k \gg 1$ we split the solution $u(x, t)$ into a ‘slow’ part $w(x, t)$ and a ‘fast’ part $\chi(kx, x, t)$. It will turn out that χ is small (of the order of $1/k^2$). Therefore we can linearise equation (24) with respect to χ . Fourier expansion with respect to the fast variable kx gives for the zero mode up to order $1/k^2$:

$$w_{tt} - w_{xx} + \sin w + \epsilon \langle \chi \cos(kx) \rangle \cos w = 0, \quad (44)$$

where the angular brackets denote spatial averaging. The resulting equation is the sine–Gordon equation with the vacuum slightly shifted. For the fundamental Fourier mode one finds the equation:

$$\chi_{tt} - \chi_{xx} + \chi \cos w + \epsilon \cos w (\chi \cos(kx) - \langle \chi \cos(kx) \rangle) + \epsilon \sin w \cos(kx) = 0. \quad (45)$$

To leading order:

$$\chi(x, t) = -\epsilon k^{-2} \sin w \cos(kx) + O(k^{-4}). \quad (46)$$

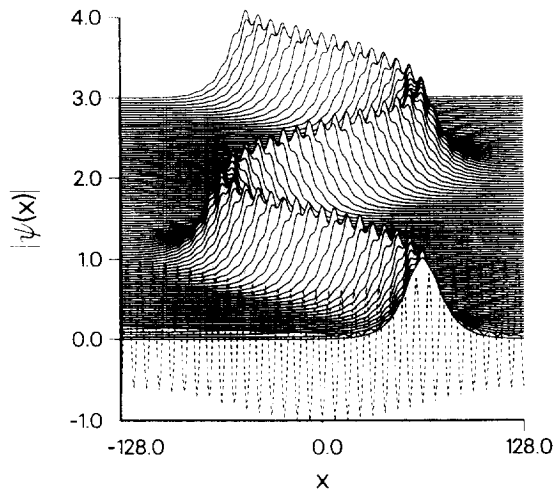


Fig. 10. Particle-like behaviour of dressed NLS solitons in a long-wavelength cosine potential being the same as in Fig. 2. The ‘fast’ perturbation has an amplitude four times as large, but is shielded completely.

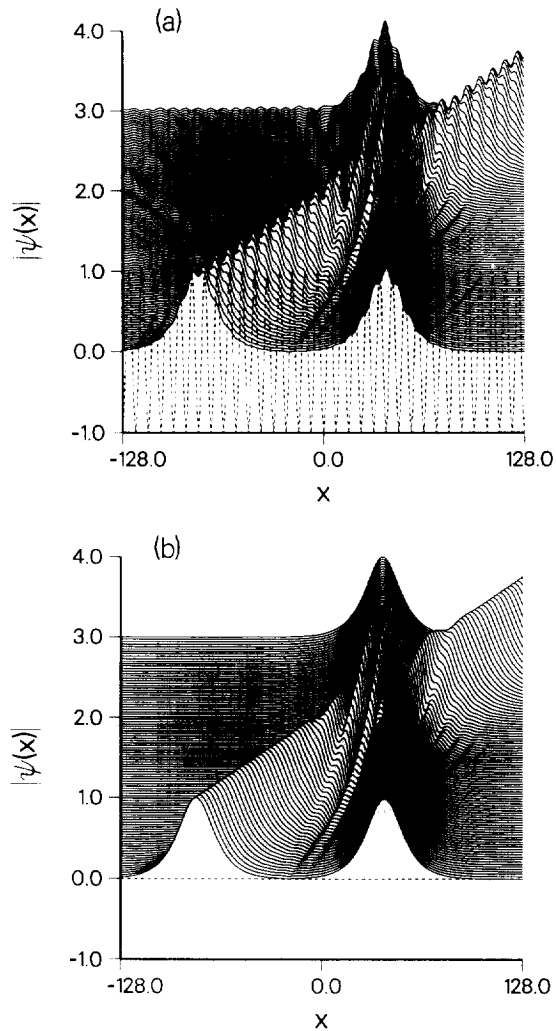


Fig. 11. Collision of two NLS solitons ($\dot{q}_1 = 0$, $\dot{q}_2 = 1.2$, $\eta_1 = \eta_2 = 0.5$). (a) Perturbed case ($\epsilon = -0.05$, $k = \pi/4$) with dressed solitons. (b) For comparison the unperturbed case with bare solitons.

This can be used to calculate:

$$\langle \chi \cos(kx) \rangle = -\frac{\epsilon \sin w}{2k^2}, \quad (47)$$

which completes the zero-mode equation:

$$w_{tt} - w_{xx} + \sin w - \frac{\epsilon^2 \sin 2w}{4k^2} = 0, \quad (48)$$

which is the so-called double sine-Gordon model [36, 37]. Like in the NLS equation the small parameter is ϵ/k . For small-amplitude breathers the similarity becomes even stronger as one approaches the NLS limit.

The dressing χ has modulations beating against the underlying perturbation, as in the NLS case for small-velocity solitons. Furthermore, the dressing is proportional to the sine of the carrier excitation. That explains why the dressing is hardly visible for weakly-perturbed kinks or antikinks, in striking contrast to breathers where the modulation is

much more pronounced. It also explains why colliding kinks and antikinks are affected by the perturbation most strongly when they are close to each other and their resulting amplitude is around $\pi/2$.

Like in the NLS case the motion of kinks, antikinks or breathers in the presence of long- and short-wavelength perturbations can be described as motion of dressed particles in a long-wavelength effective potential.

4. LENGTHSCALE COMPETITION

In this Section we address the situation of competing lengthscales, when neither the particle limit nor the dressed-particle limit apply. In this case it is not possible to distinguish a small set of collective variables which essentially slave all the other degrees of freedom. The dynamics is inherently complicated and (infinitely) many degrees of freedom are involved. We want to identify the situations in which this happens and restrict the discussion to NLS solitons and sine–Gordon breathers.

4.1. *The continuum NLS equation*

The soliton of the unperturbed NLS equation has two characteristic lengthscales, the inverse of which are the shape parameter η and the phase modulation \dot{q} (see equation (14)). Under a perturbation which has a characteristic wavenumber k (e.g. $\cos(kx)$) two situations of lengthscale competition can occur. Either we have $\dot{q} \approx k$ leading to a phase resonance, or $\eta \approx k$ leading to a shape resonance.

We first discuss the phase resonance. From equation (42) we see that the modulations of a soliton in the presence of a large- k perturbation formally diverge for $\dot{q} = k$ signalling a breakdown of the lengthscale separation ansatz. But also the numerics shows that the modulations strongly increase in size upon approaching the resonance from either side. Above the resonance the modulations are in phase with the periodic perturbation; below they beat against it. Right at the resonance the soliton quickly decays into wavetrains switching between being in phase and out of phase with the perturbation. A stable soliton propagation is no longer possible. The description of the dynamics can no longer be restricted to a few collective coordinates slaving the others. This was already illustrated in Fig. 9(b).

For $\eta \approx k$ we have the case of shape resonance. The soliton is neither sufficiently localised to move like a particle nor sufficiently extended to smooth over the potential and move like a dressed particle. Instead, it simultaneously experiences the influence of several minima and maxima of the potential which tend to split it into smaller excitations giving rise to complicated spatio–temporal behaviour. The resonance is not as sharply defined as the phase-resonance and depends on several details like the velocity of the soliton, the shape of the potential, the initial position in the case of a sudden turn-on of the potential. We illustrate the shape-resonance in Fig. 12. For further details see [35].

4.2. *The sine–Gordon equation*

Sine–Gordon breathers subject to a spatially periodic perturbation can show a shape-resonance very similar to the resonance for NLS solitons. When the breather covers only a small number of periods of the potential ($k \approx \sin \mu$) the lengthscale separation ansatz does no longer work and the breather is strongly deformed. It either radiates strongly or breaks apart into several smaller lumps distributed over the wells of the perturbing potential. Like in the NLS case the details of the decay process depend on the initial conditions like

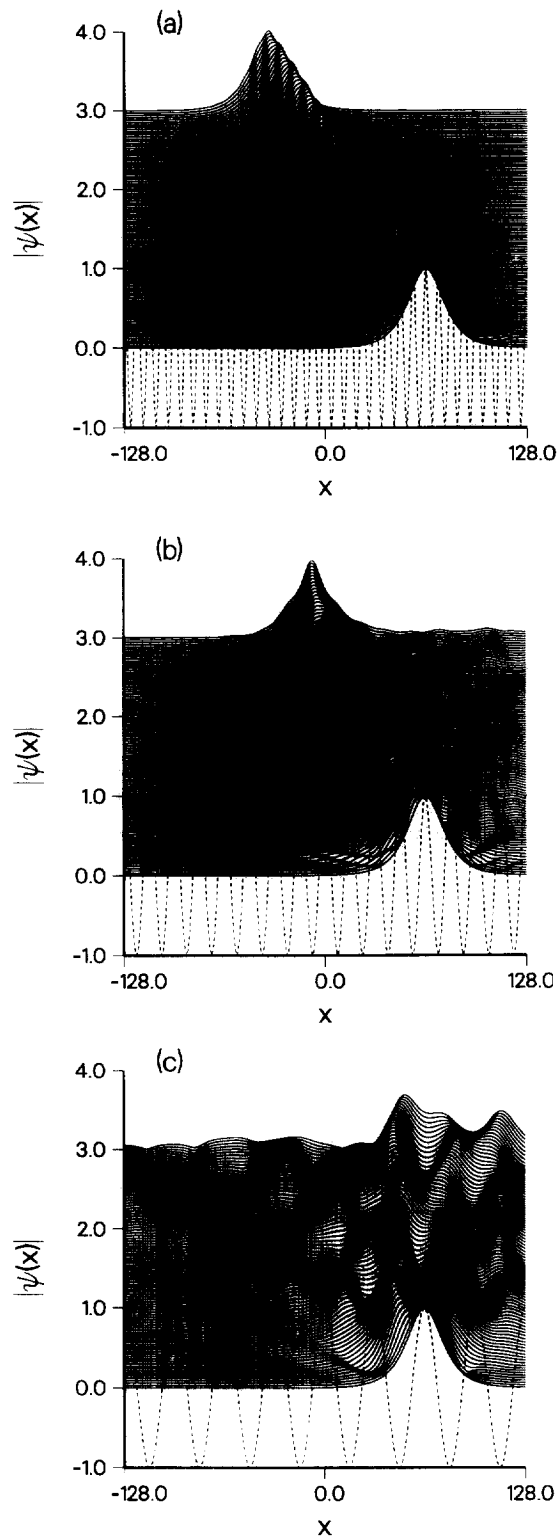


Fig. 12. Shape resonance for NLS solitons ($\eta = 0.05$, $\dot{q} = -0.04$). The amplitude of the perturbation: $\epsilon = 0.01$. The spatial period of the potential: (a) $\lambda = 8$; (b) $\lambda = 16$; (c) $\lambda = 32$.

position, phase, and velocity of the breather. We illustrate the wavenumber dependence of the process in Fig. 13. For details see [31].

When the *damped* sine-Gordon equation is subject to spatio-temporal driving, a new kind of lengthscale competition can be observed [38]. Starting from the vacuum a spatially homogeneous driving with a fixed frequency will excite a breather of a certain width. The second lengthscale is set by the spatial period of the driving. For periodic boundary conditions a third lengthscale is given by the size of the system. A rich and interesting scenario results which has been investigated by Cai *et al.* [38].

5. CONCLUSION

We have analysed the behaviour of solitary excitations in spatially-multicolour perturbations, we have determined the long-wavelength effective potential as well as the short-wavelength dressing and finally we identified the conditions for lengthscale competition. In

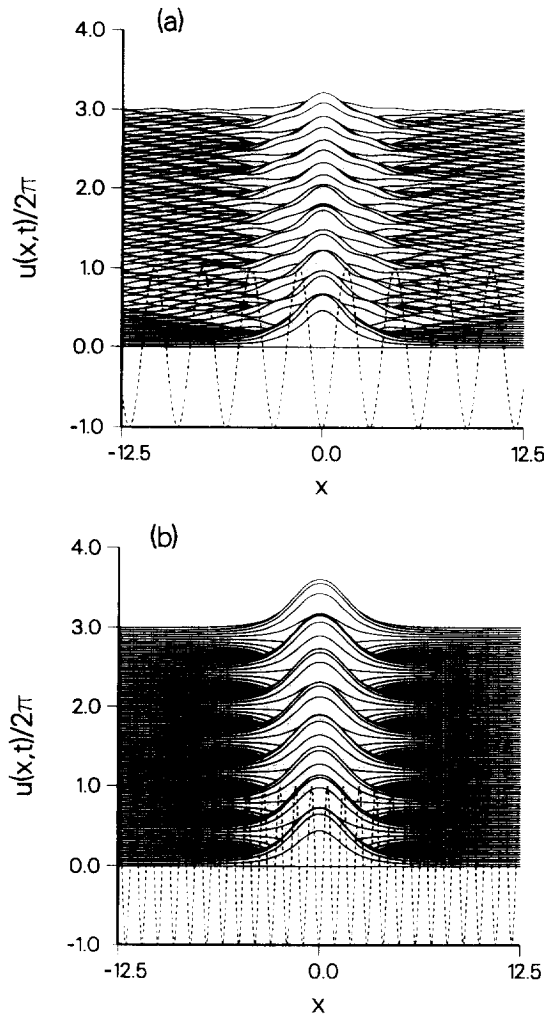


Fig. 13. Shape resonance for sine-Gordon breathers ($\mu = 1$) in a cosine potential with $\epsilon = -0.5$. (a) Lengthscale competition leading to strong radiation ($k = 2\pi/3$). (b) Breather smoothing over the short-wavelength perturbation ($k = 2\pi$).

general, lengthscale competition leads to rapid breakup of coherent excitations which has to be studied numerically.

Radiative effects have been neglected so far. They will be important at locations where the long-wavelength perturbations have large curvature. In the case of short-wavelength perturbations they will result from imperfect shielding on longer timescales or during dressed-soliton collisions. Standard perturbation theory (see [10]) has to be modified appropriately to treat the particle and dressed-particle cases.

Soliton chaos will lead to diffusive motion of solitons in collective coordinate phase-space. For $(2 + 1)$ -dimensional perturbed soliton-bearing dynamics soliton chaos can already be possible for single solitons. The far-reaching consequences of low-dimensional chaos for infinite-dimensional dynamics still have to be elucidated.

Semiclassical quantisation using collective coordinates (for literature see [14]) can be applied to solitons as well as dressed solitons in nonvanishing effective potentials. This establishes the connection with the rapidly evolving field of quantum chaos (for an overview see [39]).

Finally, the inelastic effects mentioned in 2.2 have to be analysed using the exact two-soliton solution for the NLS equation to determine the stationary distribution a dilute gas of solitons might eventually evolve to.

Acknowledgements—Most of the work presented was done in collaboration with Alan Bishop, who introduced me to this fascinating field. He deserves my major thanks. I also enjoyed working and discussing with Fadkhullah Abdullaev, Davis Cai, David Campbell, Greg Forest, Yuri Kivshar, Peter Lomdahl, Angel Sánchez and Luis Vázquez. Ed Overman generously supplied his spectral codes.

REFERENCES

1. A. R. Bishop, D. K. Campbell and St. Pnevmatikos (editors), *Disorder and Nonlinearity*. Springer Proceedings in Physics, Vol. 39. Springer, Berlin (1989); F. Kh. Abdullaev, A. R. Bishop and St. Pnevmatikos, *Nonlinearity with Disorder*. Springer Proceedings in Physics, Vol. 67. Springer, Berlin (1992).
2. A. Hasegawa, *Optical Solitons in Fibers*. Springer, Berlin (1990).
3. A. Barone and G. Paternó, *Physics and Applications of the Josephson Effect*. Wiley, New York (1982).
4. G. Grüner and A. Zettel, *Phys. Rep.* **119**, 117 (1985); *Charge Density Waves in Solids*, edited by L. P. Gor'kov and G. Grüner, Modern Problems in Condensed Matter Sciences, Vol. 25. North-Holland, Amsterdam (1989).
5. A. J. Heeger, S. Kivelson, J. R. Schrieffer and W.-P. Su, *Rev. Mod. Phys.* **60**, 781 (1988).
6. R. Blinc and A. P. Levanyuk (editors), *Incommensurate Phases in Dielectrics*, Modern Problems in Condensed Matter Sciences Vol. 14(1) North-Holland, Amsterdam (1986).
7. H.-J. Mikeska and M. Steiner, *Adv. Phys.* **40**, 191 (1991).
8. M. J. Ablowitz and P. A. Clarkson, *Solitons, Nonlinear Evolution Equations and Inverse Scattering*. Cambridge University Press, Cambridge (1991).
9. R. K. Dodd, J. C. Eilbeck, J. D. Gibbon and H. C. Morris, *Solitons and Nonlinear Wave Equations*. Academic Press, London (1982).
10. Y. S. Kivshar and B. Malomed, *Rev. Mod. Phys.* **61**, 763 (1989).
11. A. Sánchez and L. Vázquez, *Int. J. Mod. Phys.* **B5**, 2825 (1991).
12. H. Segur, *Physica* **D51**, 343 (1991).
13. Y. S. Kivshar and K. H. Spatschek, *Chaos, Solitons & Fractals* (to appear).
14. R. Rajaraman, *Solitons and Instantons*. North-Holland, Amsterdam (1982).
15. R. Boesch and C. R. Willis, *Phys. Rev.* **B42**, 6371 (1990); *Phys. Rev.* **A45**, 5422 (1992).
16. M. Salerno, *Phys. Rev.* **A46**, 6856 (1992).
17. M. J. Ablowitz and J. F. Ladik, *J. Math. Phys.* **17**, 1011 (1976).
18. R. Scharf and A. R. Bishop, *Phys. Rev.* **A43**, 6535 (1991).
19. H.-H. Chen and C.-S. Liu, *Phys. Rev. Lett.* **37**, 693 (1976).
20. A. Kosevich, *Physica* **D41**, 253 (1990).
21. L. D. Faddeev and L. A. Takhtajan, *Hamiltonian Methods in the Theory of Solitons*. Springer, Berlin (1987).
22. R. Scharf and A. R. Bishop, *Phys. Rev.* **A46**, 2973 (1992).
23. F. Kh. Abdullaev, *Phys. Rep.* **179**, 1 (1989).
24. Zhang Fei, V. V. Konotop, M. Peyrard and L. Vázquez, *Phys. Rev.* **E48**, 548 (1993).
25. Th. Dauxois, M. Peyrard, and C. R. Willis, *Phys. Rev.* **E48**, 4768 (1993).
26. R. Boesch and M. Peyrard, *Phys. Rev.* **B43**, 8491 (1991).

27. D. Campbell and M. Peyrard, *Physica* **D18**, 47 (1986).
28. Y. S. Kivshar, Z. Fei and L. Vázquez, *Phys. Rev. Lett.* **67**, 1177 (1991).
29. O. Legrand and G. Rheinisch, *Phys. Rev.* **A35**, 3522 (1987).
30. R. Scharf, Y. S. Kivshar, A. Sánchez and A. R. Bishop, *Phys. Rev.* **A45**, 5369 (1992).
31. A. Sánchez, R. Scharf, A. R. Bishop and L. Vázquez, *Phys. Rev.* **A45**, 6031 (1992).
32. A. Hasegawa and Y. Kodama, *Phys. Rev. Lett.* **66**, 161 (1991).
33. L. D. Landau and M. Lifshitz, *Mechanics*, pp. 93–95. Pergamon, London (1960).
34. Y. S. Kivshar, K. H. Spatschek, S. T. Turitsyn and M. L. Quiroga Teixeira (to be published in *Phys. Rev. A*).
35. R. Scharf and A. R. Bishop, *Phys. Rev.* **A47**, 1375 (1993).
36. C. A. Condat, R. A. Guyer and M. D. Miller, *Phys. Rev.* **B27**, 474 (1983).
37. D. K. Campbell, M. Peyrard and P. Sodano, *Physica* **D19**, 165 (1986).
38. D. Cai, A. R. Bishop and A. Sánchez, *Phys. Rev.* **E48**, 1447 (1993).
39. M.-J. Giannoni, A. Voros and J. Zinn-Justin (editors), *Chaos and Quantum Physics*, Elsevier, Amsterdam (1991).